Evolution of ferromagnetic and non-Fermi liquid state with doping: the case of Ru doped UCoGe

Michal Vališka,[1,*] Jiří Pospíšil,[2] Martin Diviš,[1] Jan Prokleška,[1] Vladimír Sechovský,[1] and Mohsen M. Abd-Elmeguid[3]

[1] *Faculty of Mathematics and Physics, Charles University, DCMP, Ke Karlovu 5, CZ-12116 Praha 2, Czech Republic*

[2] *Advanced Science Research Center, Japan Atomic Energy Agency, Tokai, Ibaraki, 319-1195, Japan*

[3] *II. Physikalisches Institut, Universität zu Köln, 0937 Köln, Germany*

arXiv:1412.8355v3 [cond-mat.str-el] 18 Jun 2015

We have investigated the impact of Ru substitution for Co on the behavior of the ferromagnetic superconductor UCoGe by performing x-ray diffraction, magnetization, specific heat and electrical resistivity measurements on polycrystalline samples of the $UCo_{1-x}Ru_xGe$ series ($0 \geq x \leq 0.9$). The initial Ru substitution up to $x \approx 0.1$ leads to a simultaneous sharp increase of the Curie temperature and spontaneous magnetization up to maximum values of $T_C = 8.6\,K$ and $M_S = 0.1\,\mu_B$ per formula unit, respectively, whereas superconductivity vanishes already for $x \approx 0.03$. Further increase of the Ru content beyond $x \approx 0.1$ leads to a precipitous decrease of both, T_C and M_S towards a ferromagnetic quantum critical point (QCP) at $x_{cr} = 0.31$. Consequently the $T - x$ magnetic phase diagram consists of a well-developed ferromagnetic dome. We discuss the evolution of ferromagnetism with x on the basis of band structure changes due to varying $5f$-ligand hybridization. This scenario is supported by the results of electronic structure calculations and consideration of the simplified periodic Anderson model. The analysis of the temperature dependencies of the electrical resistivity and heat capacity at low temperatures of the samples in the vicinity of the QCP reveals a non-Fermi liquid behavior and assigns the ferromagnetic quantum phase transition to be most likely of a continuous Hertz-Millis type.

PACS numbers: 71.10.Hf, 74.40.Kb, 71.20.Lp
Keywords: UCoGe, URuGe, Quantum critical point, non-Fermi liquid behavior, ferromagnetism

I. INTRODUCTION

The phenomena emerging near a quantum critical point (QCP) belong to the most intensively studied topics of condensed matter physics. Diligent research in this field continuously brings brand new materials carrying completely novel properties. Such progress boosts development of new theoretical approaches describing electron correlations in these systems. A specific group of those intriguing materials comprises the uranium based ferromagnetic superconductors (FM SC) UGe_2[1,2], URhGe[3] and UCoGe[4]. In these compounds superconductivity and itinerant ferromagnetism are carried by the same uranium $5f$ electrons. It is a novelty distinguishing them from previously reported $ZrZn_2$[5]. UGe_2, the first discovered case, is a model example of superconductivity (SC) induced by external pressure. Here SC appears and reaches a maximum T_{SC} on a boundary between two different FM phases under high pressure. URhGe and UCoGe are ambient pressure FM SC where both phenomena naturally coexist. A lot of effort both in theory and experiment has been done to explore the underlying mechanisms of the coexistence of FM and SC. Ferromagnetic spin fluctuations which appear in the vicinity of the QCP have been considered as the main essence for inducing unconventional spin-triplet SC state[6–8].

Quantum phase transitions (QPTs) were experimentally studied for a broad spectrum of materials like high-T_C superconductors[9], ordinary metals[10] or heavy-fermion compounds[11]. Most of such investigations have been carried out on antiferromagnets which by rule exhibit second-order QCP. Prominent examples are $CeCu_{6-x}Au_x$ with an antiferromagnetic quantum critical point (AF QCP) which is induced by chemical doping[12] or $YbRh_2Si_2$ where the AF QCP is achieved by applying external magnetic field[13]. Studies of quantum criticality in ferromagnets have been less frequent and manifest that here the situation may be much more complex. The ferromagnetic phase transition at finite Curie temperature (T_C) is by rule of a second order type. T_C of itinerant electron ferromagnets is often easily suppressed to 0 K by external pressure p or chemical composition x. However, detailed experimental investigation of archetypal ferromagnetic metals such as MnSi[10], $ZrZn_2$[5] or UGe_2[2,14] has revealed that the ferromagnetic phase is suppressed to zero temperature at a first-order transition which would mean that no QCP is observed. This can be elucidated theoretically either in terms of additional fermionic modes which may couple to the critical ferromagnetic fluctuations driving the phase transition to a first-order type[15] or that a first-order magnetic phase transition may be induced by strong magneto-elastic coupling[16]. No generic scenario can be drawn for the QPTs of the above mentioned materials because of rather individually different phenomena appearing in the quantum critical region. In particular MnSi becomes long-period helimagnet (showing ferromagnetism only locally) in which the thermal phase transition is weakly first-order[17], UGe_2 exhibits strong uniaxial anisotropy[18] and $ZrZn_2$ exhibits a marginal Fermi liquid ground state[19].

UCoGe, the subject of the present study, is unique in the group of FM SC due to the much lower energy

scale on which the magnetism appears[20]. The low Curie temperature of UCoGe is only 3 K[4,21] together with the tiny spontaneous magnetization of $0.03\,\mu_B$ per formula unit (f.u.) indicate that UCoGe is close to a ferromagnetic instability[22]. It has been observed, however, that the Ru and Fe substitution for Co rapidly stabilizes the ferromagnetic state[23], despite the fact that URuGe and UFeGe behave like Pauli paramagnets down to the lowest temperatures[24]. Similar increase of T_C was reported in the case of the initial substitution of Co and Ru for Rh in URhGe[25,26] with the development of a non-Fermi liquid (NFL) state on the higher doping boundary of the FM dome[26]. These observations motivated us to inspect the development of the magnetic as well as electrical and thermal transport properties in the $UCo_{1-x}Ru_xGe$ series over the entire concentration range ($0 \geq x \leq 0.9$). Our study is based on extensive investigation of the crystal structure, magnetization, AC magnetic susceptibility, specific heat and electrical resistance of numerous polycrystalline samples with various Ru content. The results are discussed and compared with theoretical calculations and related models considering the leading role of the $5f$-ligand hybridization.

II. EXPERIMENTAL DETAILS

In order to study the development of the magnetic state in the $UCo_{1-x}Ru_xGe$ system we have prepared a series of polycrystalline samples with different Ru concentrations x between 0 and 0.9. All samples were prepared by arc-melting of the stoichiometric amounts of the elements (purity of Co 4N5, Ge 6N and Ru 3N5). U was purified by the Solid State Electrotransport technique (SSE)[27] following previous experience with preparation of UCoGe[27]. The arc melting process was realized under protective Ar (6N purity) atmosphere on a water cooled Cu crucible. Each sample was three times turned upside down and subsequently re-melted in order to achieve the best homogeneity. All samples were separately wrapped into a Ta foil (99.99%), sealed in a quartz tube under the vacuum of $1{\cdot}10^{-6}$ mbar , subsequently annealed at 885 °C for 14 days and then slowly cooled down to room temperature to avoid creation of the internal stresses. Each sample was characterized by X-ray powder diffraction (XRPD) at room temperature on a Bruker D8 Advance diffractometer. The obtained data were evaluated by Rietveld technique[28] using FullProf/WinPlotr software[29,30] with respect to the previously published crystallographic data of the UCoGe[31] and URuGe[24] compound. The chemical composition of our samples was verified by a scanning electron microscope (SEM) Tescan Mira I LMH equipped with an energy dispersive X-ray detector (EDX) Bruker AXS. Samples were afterward properly shaped for individual measurements with a fine wire saw to prevent induction of additional stresses and lattice defects. The electrical resistivity (ρ) was measured by the 4-probe method on bar-shape samples ($1 \times 0.5 \times 4\,\mathrm{mm}^3$) and heat-capacity ($C_p$) measurements were performed on thin plates ($2 \times 2 \times 0.2\,\mathrm{mm}^3$) by the relaxation method on PPMS9T and PPMS14T devices using a ^{3}He insert. Magnetization (M) measurements were done on cubic samples ($2 \times 2 \times 2\,\mathrm{mm}^3$) using a MPMS7T device. The magnetization was evaluated in μ_B/f.u.. For simplicity we omit "/f.u." everywhere throughout the paper.

The electronic structure calculations were performed on the basis of the density-functional theory (DFT) within the local-spin-density approximation (LSDA)[32] and the generalized gradient approximation (GGA)[33]. For this calculations we have used the full-potential augmented-plane-wave together with the local-orbitals method (APW+lo) as a part of the latest version (WIEN2k) of the original WIEN code[34].

III. RESULTS

A. X-ray diffraction

Both UCoGe and URuGe crystalize in the orthorhombic TiNiSi-type structure (space group Pnma)[24,31] with the room-temperature cell parameters $a = 6.852$ Å, $b = 4.208$ Å, $c = 7.226$ Å and $a = 6.678$ Å, $b = 4.359$ Å, $c = 7.539$ Å, respectively[24,31]. The unit cell volume of UCoGe ($V = 208.3\,\text{Å}^3$)[31] is about 5% smaller than that of the URuGe compound ($V = 219.5\,\text{Å}^3$)[24]. The XRPD patterns confirmed the orthorhombic TiNiSi-type structure of samples over the entire concentration range of the $UCo_{1-x}Ru_xGe$ series.

The evaluated lattice parameters are listed in Table I. The concentration dependence of all three lattice parameters and the unit volume reveals a linear behavior, i.e. obeying Vegard's law[35] (see Fig. 1).

While the lattice parameters b and c increase with increasing x, the lattice parameter a simultaneously decreases. The volume expansion seems to reflect the increase of the covalent radii from Co (126 pm) to Ru (146 pm)[36]. Refinement of the diffraction patterns showed, that the Ru atoms really substitute the Co ones on their sites.

Although the unit cell volume expands with increasing Ru concentration the distance between the nearest-neighbor U ions d_{U-U} contracts (see Fig.1). This result is not surprising because the d_{U-U} lines form a chain meandering along the a-axis.

B. Magnetization and AC-Susceptibility

We have measured the magnetization of each sample as a function of temperature and applied magnetic field. The values of M_S have been estimated from the magnetization curves measured at 1.85 K (the lowest available temperature in our MPMS7T) by extrapolating the magnetization from high magnetic fields to 0 T.

Table I. The lattice parameters and the unit cell volume of the $UCo_{1-x}Ru_xGe$ samples as obtained from the refinement of the X-ray powder diffraction patterns.

x	a (Å)	b (Å)	c (Å)	V (Å^3)
0.10	6.8344	4.2188	7.2717	209.6671
0.20	6.8216	4.2267	7.3048	210.6173
0.21	6.8204	4.2261	7.3026	210.4879
0.22	6.8189	4.2279	7.3079	210.6840
0.23	6.8178	4.2272	7.3085	210.6325
0.24	6.8131	4.2280	7.3145	210.6999
0.25	6.8150	4.2320	7.3229	211.2003
0.26	6.8269	4.2385	7.3347	212.2355
0.27	6.8203	4.2363	7.3314	211.8247
0.28	6.8205	4.2390	7.3392	212.1890
0.29	6.8133	4.2373	7.3389	211.8711
0.30	6.8077	4.2373	7.3413	211.7662
0.40	6.7880	4.2454	7.3704	212.3984
0.50	6.7709	4.2577	7.4046	213.4669
0.60	6.7522	4.2710	7.4416	214.6050
0.70	6.7336	4.2868	7.4741	215.7451
0.80	6.7137	4.3015	7.5041	216.7105
0.90	6.6909	4.3212	7.5290	217.6849

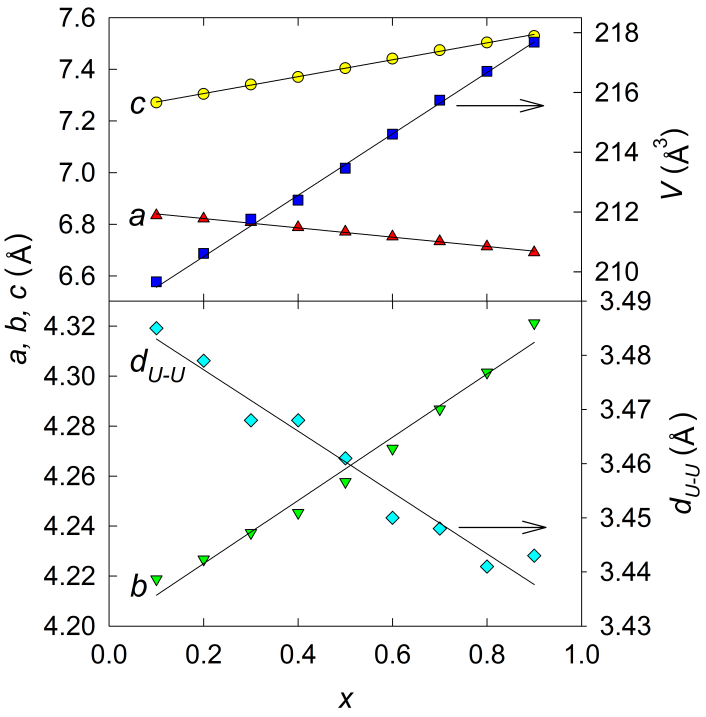

Figure 1. (Color online) - Concentration dependence of the lattice parameters and the unit cell volume of the $UCo_{1-x}Ru_xGe$ samples. The lines serve as guides to the eye.

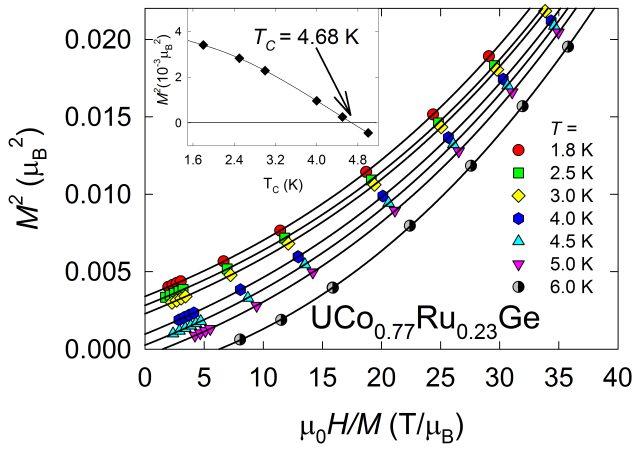

Figure 2. (Color online) - Arrott plots for the $UCo_{0.77}Ru_{0.23}Ge$ compound. Solid lines are the third order polynomial functions. The inset shows that T_C is taken as the value for which the intersection with the M^2 axis would be zero.

The values of T_C have been determined by several methods. Arrott plot analysis of magnetization data is widely considered as the most reliable method[37]. For this purpose the magnetization curves were measured at several temperatures in the vicinity of the expected T_C. The Arrott plots obtained from our magnetization data are strongly nonlinear. These curves can be approximated by a third degree polynomial function (see a model example in Fig. 2). T_C is determined as the temperature of the Arrott plot isotherm that would cross the M^2 axis at 0. An example of the relevant construction is shown in the inset of Fig. 2.

The nonlinearity of the Arrott plots (the cubic M^2 vs H/M dependence) suggests presence of a magnetization component linearly dependent on the magnetic field. This is related to the fact that UCoGe and the other UTX compounds crystallizing in the orthorhombic TiNiSi-type structure exhibit strong uniaxial anisotropy with easy magnetization direction along the c-axis. The hard magnetization directions within the $a-b$ plane are characteristic by a weak temperature-independent paramagnetic response with the magnetization proportional to the magnetic field. We have observed the same type of magnetocrystalline anisotropy for the ferromagnetic $UCo_{1-x}Ru_xGe$ single crystals which we have grown as a part of another study (see Ref.[38]). Consequently the polycrystalline samples should show a corresponding linear component also in the ferromagnetic state. By subtracting a suitable linear term from measured magnetization data we obtain the corrected magnetization values $M^* = M - a \cdot \mu_0 \cdot H$. For $a = 0.006\,\mu_B \cdot T^{-1}$ the Arrott plots M^2 vs H/M^* are indeed linear except the low-field part due to low-field magnetization processes and influence of a demagnetization field as can be seen for example in the case of the $UCo_{0.77}Ru_{0.23}Ge$ sample in Fig. 3.

The obtained T_C and M_S values are listed for all samples in Table II and plotted in the complex phase diagram in Fig. 9(a). T_C steeply increases with the initial Ru substitutions for Co which is in agreement with the results published in previous work[23]. This trend terminates at

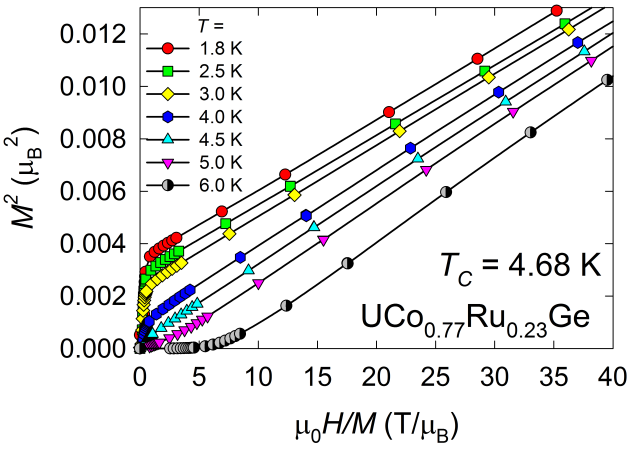

Figure 3. (Color online) - Revised Arrott plots after subtraction of the linear term with the slope $a = 0.006\,\mu_B \cdot T^{-1}$ from the magnetization data measured on the $UCo_{0.77}Ru_{0.23}Ge$ sample.

$x_{max} \approx 0.1$ where the ordering temperature reaches a maximum value of $T_{C,max} \approx 8.6$ K. This value is almost three times higher than $T_C = 3$ K of the parent compound[4] and is comparable with the value found by Huang et al. in the case of the corresponding substitution of Fe for Co in UCoGe[39]. Increasing Ru concentration beyond $x \approx 0.1$ is accompanied by a simultaneous decrease of T_C and M_S towards zero at the critical concentration $x_{cr} \approx 0.31$. Thus, the ferromagnetic dome of the concentration dependence of T_C in the $T - x$ magnetic phase diagram is intimately connected with a corresponding change of M_S (see Fig. 9(a)).

The $M(T)$ curves measured on selected samples with concentration above $x \geq 0.1$ displayed in Fig. 4 also manifest the collapse of ferromagnetism with increasing Ru content. The estimated T_C values as derived from the temperature of the inflection point in the $M(T)$ dependence (measured in low external field of 10 mT) are in good agreement with ordering temperatures obtained from the Arrott plot analysis (see Table II and Fig. 9 (a)).

We have also measured the AC magnetic susceptibility (χ) for different Ru concentration above $x \geq 0.21$ at temperatures down to 1.85 K using a MPMS device. For measurements at lower temperatures (down to 400 mK) a custom-made coil system attached to the ^{3}He insert in PPMS and a lock-in amplifier were utilized (the same setup as that used in Ref.[40]). T_C is usually identified as the temperature of the maximum of the real part of χ (see Fig. 5). While the low temperature AC susceptibility of the sample with $x = 0.29$ reveal a well-developed peak at 1.44 K indicating the onset of ferromagnetism, no clear peak maximum is observed for the sample with $x = 0.30$, which might be at approximately 350 mK as the lowest-T point was measured at 400 mK. For the sample with $x = 0.31$ no trace of χ anomaly has been detected down to 400 mK which seems to be in the immediate vicinity of the critical Ru concentration for existence of ferromagnetism in the $UCo_{1-x}Ru_xGe$ compounds.

Table II. Values of the spontaneous magnetization M_S and Curie temperature derived from Arrott plot analysis ($T_{C,Arrott}$), temperature dependence of AC susceptibility ($T_{C,\chi}$), magnetization ($T_{C,M}$) and specific heat (T_{C,C_p}), and Sommerfeld coefficient (γ) as determined from the specific heat data at low temperatures for samples with various concentration of Ru (x).

x	M_S (μ_B)	$T_{C,Arrott}$ (K)	$T_{C,\chi}$ (K)	$T_{C,M}$ (K)	T_{C,C_p} (K)	γ ($\frac{mJ}{mol \cdot K^2}$)
0	0.0300	-	-	2.50	-	-
0.01	0.0330	4.20	-	4.00	-	-
0.05	0.0750	8.30	-	7.50	-	-
0.10	0.1060	8.62	-	8.20	8.60	0.0861
0.20	0.0540	5.70	-	5.40	5.70	0.1066
0.21	0.0580	5.70	5.20	5.40	5.90	0.1100
0.22	0.0594	5.01	4.70	5.00	5.30	0.1133
0.23	0.0568	4.68	4.20	4.60	4.30	0.1152
0.24	0.0270	3.55	3.50	3.60	3.80	0.1258
0.25	0.0300	3.49	3.40	3.40	3.30	0.1333
0.26	0.0213	2.51	2.80	2.80	3.00	0.1353
0.27	0.0223	2.77	2.40	2.60	2.80	0.1435
0.28	0.0219	2.32	1.90	2.30	2.70	0.1405
0.29	0.0077	-	1.44	-	1.40	0.1529
0.30	0.0013	-	$\approx .35$	-	-	0.1598
0.40	0.0011	-	-	-	-	0.1523
0.50	0.0001	-	-	-	-	0.1490

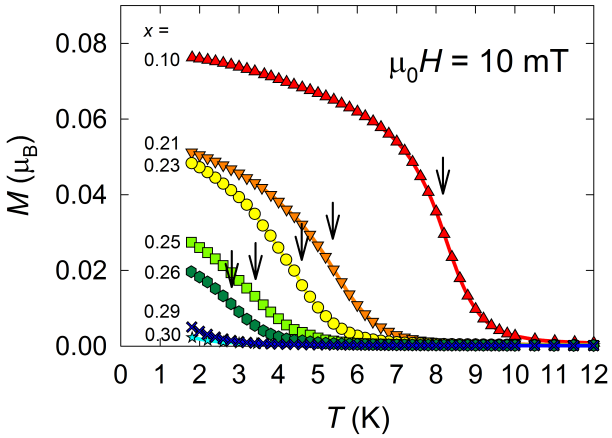

Figure 4. (Color online) - Temperature dependence of the magnetization of selected $UCo_{1-x}Ru_xGe$ compounds measured in an external magnetic field of 10 mT. The arrows mark T_C for each composition.

C. Specific heat

To analyze the different contributions to the specific heat we have subtracted from experimental data the phonon contribution using the fit of the phonon specific heat as a $C_{ph}(T) = \beta T^3$. We typically obtain values of

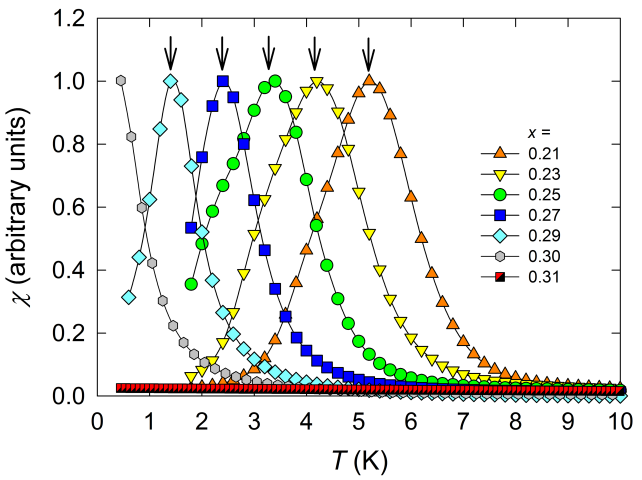

Figure 5. (Color online) - Temperature dependence of the real part of the AC susceptibility of selected $UCo_{1-x}Ru_xGe$ compounds. The arrows mark T_C for each composition. Data are plotted in arbitrary units and normalized because the home made coil for measurement in ^{3}He (used for measurement of samples with $x = 0.29 - 0.31$) provides only relative data. Some curves are not shown for clarity of the figure.

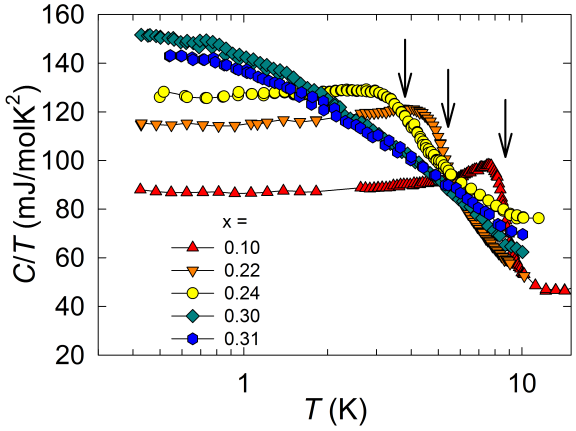

Figure 6. (Color online) - C/T versus log$T$ plot for selected $UCo_{1-x}Ru_xGe$ compounds. Black arrows indicate T_C for samples with $x = 0.10$, 0.22 and 0.24, respectively.

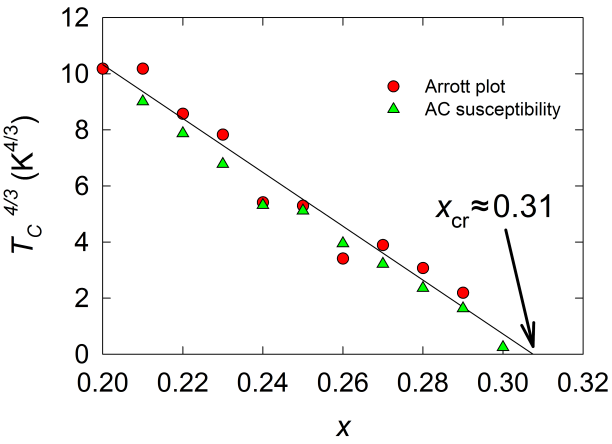

Figure 7. (Color online) - Estimation of the critical concentration for ferromagnetism in the $UCo_{1-x}Ru_xGe$ system by applying the $T_C^{4/3}$ vs x plot and the T_C values derived from the Arrott plots.

$\beta \approx (0.52 - 0.56) \cdot 10^{-3}\,\mathrm{J \cdot mol^{-1}K^{-4}}$ which correspond to Debye-temperature values of $151 - 155\,\mathrm{K}$. The remaining part of the specific-heat C represents the sum of the electronic and magnetic contributions C_e and C_m, respectively.

Fig. 6 displays the specific heat C divided by temperature T versus T on a log scale for selected samples between $x = 0.1$ and 0.31. The anomaly at T_C is gradually smeared out and shifted to lower temperatures with increasing Ru concentration. Samples with $x \leq 0.3$ show clear anomalies that are coincident with the onset of ferromagnetic order and are in reasonable agreement with the T_C values derived from magnetization and AC susceptibility (see Table II and Fig. 9 (a)). For samples with $x = 0.30$ and 0.31 C/T versus log$T$ exhibits nearly linear dependence between 1 and $\sim 10\,\mathrm{K}$ but gradually levels off at lower temperatures. This indicates a non-Fermi-liquid (NFL) behavior $C(T)/T = c\ln(T_0/T)$[41,42] that is expected for concentrations in the vicinity of the ferromagnetic QCP. We note that our data do not follow this dependence in the whole temperature range similar to that recently reported on $UCo_{1-x}Fe_xGe$ system[39].

We further calculate the magnetic entropy S_m integrated over the temperature range from 0.7 K up to the T_C for each sample and find a steady decrease of S_m with increasing x from $0.13\,\mathrm{R\ln 2}$ for $x = 0.1$ down to $0.006\,\mathrm{R\ln 2}$ at $x = 0.30$ (see Fig. 9(c)). This is consistent with the observation of a gradual disappearance of the itinerant magnetic moment by approaching the QCP ($x_{cr} \approx 0.31$). As the system approaches the critical concentration we observe a large increase of the value of Sommerfeld coefficient γ with a maximum near $x_{cr} \approx 0.31$ which reflects an enhancement of the effective mass of the quasiparticles in the region where ferromagnetism is suppressed. This finding is consistent with the presence of a strong spin fluctuation near the ferromagnetic QCP. According to the prediction for the dependence of T_C on a control parameter (x) for itinerant ferromagnets QCP by Millis and Hertz[41,42] the ordering temperature should obey the relation $T_C \sim (x_{cr} - x)^{3/4}$[43] i.e. a linear $T_C^{4/3}$ vs x plot. As we show in Fig. 7 a linear fit of T_C values for the samples with x from 0.2 to 0.3 reveals that T_C vanishes at the critical concentration $x_{cr} \approx 0.31$ consistent with this model.

D. Electrical resistivity

The low-temperature resistivity data measured on selected polycrystalline samples are plotted in Fig. 8.

Anomalies connected with the transition from paramagnetic to ferromagnetic state are not clearly visible. It is evident, that increasing Ru content leads to considerable changes of the low temperature resistivity behavior. The $\rho(T)$ data below T_C reasonably follow the $\rho = \rho_0 + AT^2$ dependence usual for ferromagnets. Data above T_C were fitted to the relation:

$$\rho = \rho_0 + AT^n \tag{1}$$

The inflection point of the $\rho(T)$ dependence was taken as an upper limit for the fitting. The exponent (n) gradually decreases as the Ru content approaches the critical concentration x_{cr}. The minimum value of $n \approx 1.13$ for $x = 0.31$ is close to the proposed linear temperature dependence from the theory of Millis and Hertz[41–43] for NFL behavior of a clean 3-dimensional itinerant ferromagnets rather than to the scaling with the exponent $n = 5/3$ which follows from the spin-fluctuation theory of Moriya[43]. The samples with higher concentration of Ru ($x > x_{cr}$) seem to exhibit gradual recovery towards a FL state which is documented by increasing the value of n exponent with increasing x above x_{cr}.

Development of the exponent n is summarized in the $T - x$ phase diagram (Fig. 9 (b)). In order to see the exponent n as a function of temperature we have calculated the logarithmic derivative of the electrical resistivity according to the Eq. (2).

$$n = \frac{\mathrm{d}\ln(\rho - \rho_0)}{\mathrm{d}\ln T} \tag{2}$$

The results of this analysis are displayed in the colored part of the phase diagram in Fig. 9 (a). One can see a significant change of the exponent between the region of ferromagnetic ordering ($T < T_C$) where $n = 2$ and in the nonmagnetic state where $n < 2$. The sharp decrease of the value n near x_{cr} down to the lowest temperatures is surrounded by regions of higher n (rapidly increasing on the FM side for $x < x_{cr}$ and slower increase on the paramagnetic side).

E. Theoretical calculations

In order to better understand the changes in the electronic structure of the $UCo_{1-x}Ru_xGe$ compounds across the ferromagnetic QCP, we have performed first-principles theoretical calculations on the paramagnetic compound URuGe. As a matter of fact, while the density of states (DOS) of the parent compound UCoGe is known (Ref.[45]) the information about the DOS of URuGe are missing. The calculated total and partial DOS of the URuGe are plotted in Fig. 10.

We used the calculated URuGe band structure by considering the simple model of Silva Neto et al.[46] which is

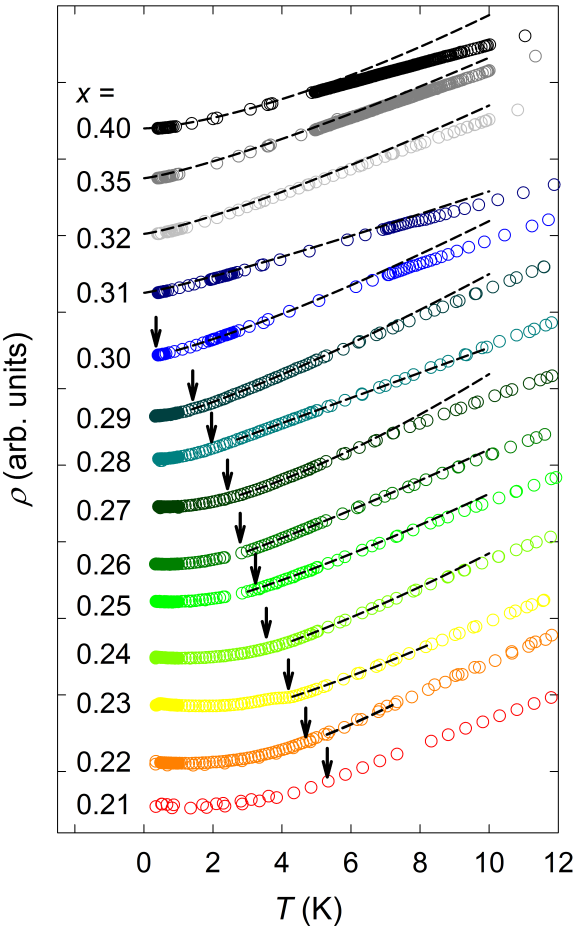

Figure 8. (Color online) - Temperature dependence of the electrical resistivity for selected polycrystalline samples of $UCo_{1-x}Ru_xGe$. The vertical arrows denote T_C values obtained from AC susceptibility data. Dashed lines are fits to data above T_C according to Eq. (1). Each curve is arbitrary vertically shifted for better clarity of the figure.

based on the periodic Anderson model[47,48]. This simplified model proposes the key role of the $nd-5f$ hybridization (V_{df} in Eq. (3)), where n is the number of d electrons in the observed non-monotonous evolution of T_C in the $URh_{1-x}Co_x$ system. They described the evolution of T_C with increasing x as a consequence of the broadening of the nd and $5f$ bands (W_d, W_f), respectively, and the mutual shift of their centers ($C_{Td} - C_{Uf}$) that are related as[46]:

$$V_{df} = \frac{W_d W_f}{C_{Td} - C_{Uf}} \tag{3}$$

If we apply this model to our $UCo_{1-x}Ru_xGe$ system we can qualitatively describe the non-monotonous evolution of T_C with Ru concentration. The concentration dependence of the broadness of the nd band is assumed to be linear according to 4

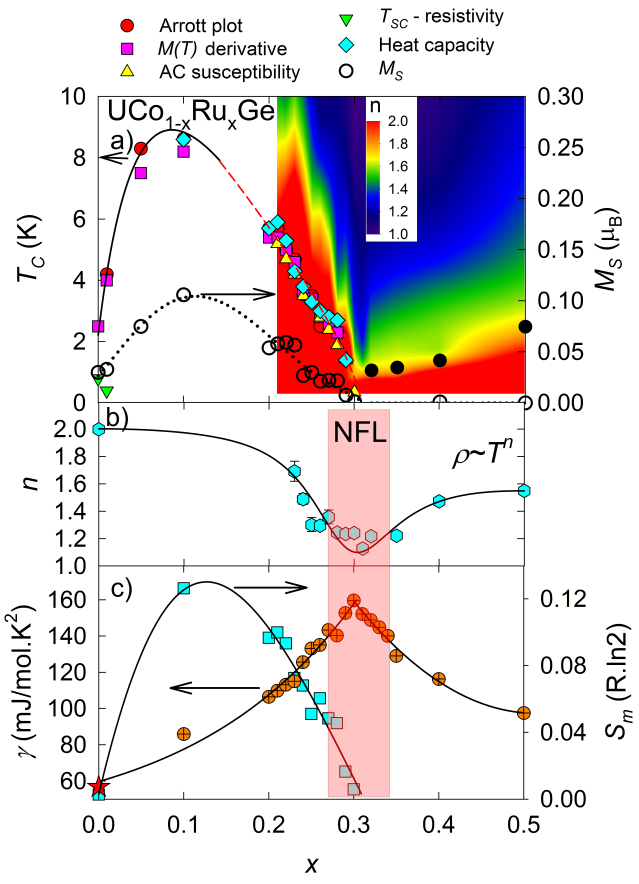

Figure 9. (Color online) - Panel a) shows the $T-x$ phase diagram based on measurements of polycrystalline samples. The diagram is supplemented by the results of the electrical resistivity measurement revealing occurrence of superconductivity in the parent UCoGe compound and in $UCo_{0.99}Ru_{0.01}Ge$ - the two data points are taken from Ref.[23] (green triangle). The black solid line is only guide to the eye while the red dashed part is a fit of $T_C \sim (x_{cr}-x)^{3/4}$. The right axis denotes the spontaneous magnetization M_S (dashed line in the plot is only a guide to the eye). The color plot shows local exponents of the resistivity obtained as $n = \frac{d\ln(\rho-\rho_0)}{d\ln T}$. The black filled circles show the temperature where resistivity starts to deviate from the T^2 dependence. Panel b) shows the evolution of the coefficients n from the fitting of the low temperature dependence of the electrical resistivity with equation $\rho = \rho_0 + AT^n$ for $T > T_C$. The right vertical axis shows $RRR = \rho_{300\,K}/\rho_{0.4\,K}$ as a function of x. Panel c) shows development of C/T (extrapolated to 0 K) and the magnetic entropy S_m (value for the parent UCoGe is taken from Ref.[44] and is marked by a star).

$$W_d(x) = W_d^{Co}(1-x) + W_d^{Ru}(x) \qquad (4)$$

where $W_d^{Co} = 6.1\,\text{eV}$(Ref.[45]) and $W_d^{Ru} = 8.7\,\text{eV}$ (see Fig. 10) and $W_f = 0.43\,\text{eV}$ (Ref.[45]). Such a behavior is consistent with other UTX (T= transition metal, $X = p$ element) compounds where the d band broadens while we move from the $3d$ to the $4d$ transition metals[49].

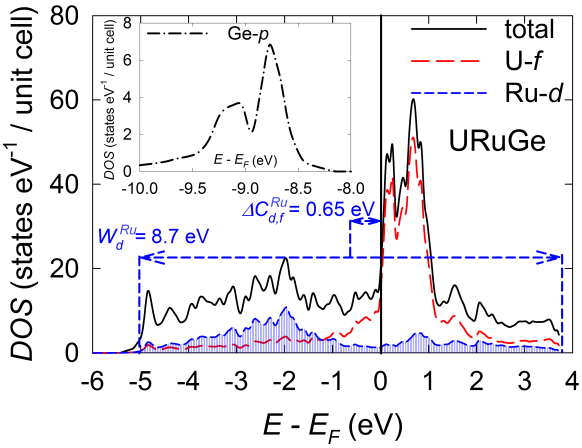

Figure 10. (Color online) - Total and partial density of states (DOS) for U–f states and Ru–d states in URuGe. Width of the d-band (W_d^{Ru}) and its center ΔC_{df}^{Ru} are marked by dashed arrows. Inset shows that the contribution of the Ge–p states is far from the Fermi level.

Consequently $(C_{Td} - C_{Uf})(x) = \triangle C_{df}(x)$ deviates from linearity

$$\Delta C_{df}(x) = \Delta C_{df}^{Co}(1-x) + \Delta C_{df}^{Ru}(x) + \delta'' x^2(1-x) + \delta''' x(1-x)^2 \qquad (5)$$

We used the values from calculated DOSes, i.e. $\Delta C_{df}^{Ru} = 0.65\,\text{eV}$ and $\Delta C_{df}^{Co} = 1.5\,\text{eV}$ (Ref.[45]) and adjustable parameters were taken as $\delta'' = 2\cdot10^{-5}$ and $\delta''' = 2$. Such an approach leads to a non-monotonous dependence of the $d-f$ hybridization term V_{df}; starting with $V_{df}(x=0) \approx 1.73$ for UCoGe (in agreement with Ref.[46]), $V_{df}(x=1) \approx 5.55$ for URuGe and $V_{df}(x \approx 0.3) \approx 1.9$ as estimated for the ferromagnetic QCP[46]. The overall $V_{df}(x)$ dependence starts with its decrease and thereby causes an enhancement of the density of f states at the Fermi level $N_f(E_F)$[50]. In case of itinerant ferromagnets we can estimate the ordering temperature as a function of the density of states at the Fermi level $T_C \sim (IN(E_F)-1)^{3/4}$ where I is the Stoner integral and $N(E_F)$ is the total density of states at the Fermi level[51]. In this respect we can attribute the initial increase of T_C to the enhanced $N(E_F)$. At $x \approx 0.07$ the $d-f$ hybridization reaches its minimum value $V_{df} = 1.7$ and starts to increase with increasing x. This point qualitatively corresponds to the position of the maximum T_C in the experimental data at $x \approx 0.1$. As the Ru concentration increases the d-band is shifted closer to the position of the f-band and the hybridization increases and thereby results in a reduction of the contribution of the $N_f(E_F)$ to $N(E_F)$[50]. For the reason mentioned above the ordering temperature decreases and reaches zero near $x_{cr} \approx 0.31$.

IV. DISCUSSION

The $5f$ electron magnetism in uranium compounds is controlled by the degree of overlap of the $5f$ wave functions of neighboring U ions and by the hybridization of the U-ion $5f$-electron states with states of the ligand valence electrons ($5f$-ligand hybridization). These two mechanisms cause that the $5f$-electron orbitals loose their atomic character which they exhibit in the U free ion. Thus, the $5f$-$5f$ overlap and/or strong $5f$-ligand hybridization lead to delocalization of the $5f$-electrons, their participation in metallic bonding[52], and consequently a washout of the U magnetic moment[53]. In addition, the spin-orbit interaction in the U ion plays an important role in electronic structure. Accordingly, an orbital magnetic moment antiparallel to the spin moment is induced by the strong spin orbit coupling in the spin-polarized energy bands of itinerant $5f$ electron materials[54,55]. The magnitude of the U $5f$-electron magnetic moments is thus further strongly reduced due to the mutual compensation of the orbital and spin components. The orbital moment is by rule larger than the spin moment considering results of so far done relevant experiments (see relevant references in Ref.[56]).

On the other hand, the $5f$-ligand hybridization plays a dual role in U compounds. Besides washing out the $5f$-electron magnetic moment it mediates an indirect exchange interaction which couples the uranium magnetic moments to promote the magnetic ordering and simultaneously causes very strong magnetocrystalline anisotropy even in very weak itinerant magnets[56,57]. Within this process the hybridized ligand valence states become polarized and as a result the ligand ion (especially transition element ion) exhibits a small induced magnetic moment which is usually parallel to the dominant $5f$-electron orbital component (see relevant references in Ref.[56]). This scenario apparently holds for UCoGe as evidenced from a recent X-ray magnetic circular dichroism (XMCD) study[58] and polarized neutron diffraction (PND) experiments on $UCo_{0.97}Ru_{0.03}Ge$ and $UCo_{0.88}Ru_{0.12}Ge$ single crystals[38]. These experiments confirm that the $5f$-electron orbital moment dominates the antiparallel spin component. A much smaller Co magnetic moment is induced by the $5f$-$3d$ hybridization.

Considering the change of the U-U distance $d_{\mathrm{U-U}}$ between the nearest U neighbor ions (overlap of $5f$ orbitals) within the $UCo_{1-x}Ru_xGe$ series, we find that $d_{\mathrm{U-U}}$ decreases with increasing Ru concentration from ≈ 3.48 Å in UCoGe to 3.44 Å in URuGe (see Fig. 1 and Fig. 11). Both values fall rather on the "nonmagnetic side" of the Hill plot[59]. On the other hand one should bear in mind that each U ion has only 2 nearest U neighbors on the $d_{\mathrm{U-U}}$ chain meandering along the a-axis. If the $5f$-$5f$ overlap was the only mechanism controlling magnetism then a gradual washout of U magnetic moment and monotonously decreasing of T_{C} with increasing Ru content would be expected. On the contrary, however, we observe an initial rapid increase of T_{C} to a maximum followed by a suppression of ferromagnetism with further increasing x. We note that our observation of a ferromagnetic dome in magnetic phase diagram in $UCo_{1-x}Ru_xGe$ (see Fig. 9 (a)) is similar to those observed for $UCo_{1-x}Fe_xGe$[39], $URh_{1-x}Ru_xGe$[26] and $URh_{1-x}Co_xGe$[25].

Apparently an additional mechanism, namely the $5f$-ligand hybridization must be taken into account for conceiving the complex evolution of ferromagnetism in these systems. The increase of T_{C} and U magnetic moment with increasing x up to 0.12 is accompanied by increasing the $5f$ electron orbital moment[38]. The increase of the orbital moment is usually considered as a sign of partial localization of $5f$ electrons because the orbital moment density is distributed closer to the nucleus than the spin density as it has been demonstrated on a detailed study of the U $5f$ electron form factor in UFe_2[55,60]. Nevertheless, the μ_L/μ_S ratio of ≈ 2.3 indicates still a significant delocalization of the $5f$ electron states for $x = 0.12$[38]. As we mention above our theoretical band structure calculation provide the basis for understanding the mechanism responsible for the ferromagnetic dome in the magnetic phase diagram of $UCo_{1-x}Ru_xGe$ by following the simple model treating the changes of $5f - nd$ hybridization with variations of the widths and mutual positions on the energy scale of the transition metal d bands and U $5f$ bands[46]. Accordingly, the non-isoelectronic substitution of Co by Ru causes broadening of the d band from $3d$ to the $4d$ transition metal-like. Together with the mutual movement of the d and f bands on energy scale itself we can qualitatively conceive the dome-like dependence of the ordering temperature T_{C}. This is an important confirmation of the trend. Variations of the $5f - nd$ hybridization most likely cause analogous non-monotonous variation of the magnetic ground state of $UCo_{1-x}Fe_xGe$[39] and $URh_{1-x}Ru_xGe$[26] exhibiting also a ferromagnetic dome in the magnetic phase diagram. It is worth to mention that the non-monotonous evolution of magnetic ground state causing a ferromagnetic dome in the magnetic phase diagram is not only specific to the $UTGe$ compounds possessing the orthorhombic TiNiSi-type structure. Analogous trends reflecting the varying $5f - nd$ hybridization are observed also in UTX compounds with the hexagonal ZrNiAl-type structure. Here UFeAl[61], URuAl[62] and UCoAl[63] are paramagnets. The latter compound is, however, close to a ferromagnetic instability. A magnetic field of only 0.6 T induces in UCoAl itinerant electron metamagnetism[64,65]. URhAl[62] and URhGe[56] are ferromagnets. Ferromagnetic domes are observed in the magnetic phase diagrams of $UCo_{1-x}Ru_xAl$[66], $URh_{1-x}Ru_xAl$[67], $URh_{1-x}Ru_xGa$[67] and anticipated from the results reported on $UCo_{1-x}Fe_xAl$[68].

The observed strong delocalization of the $5f$ electrons in $UCo_{1-x}Ru_xGe$ at higher Ru concentrations is reflected by a dramatic decrease of the magnetic entropy S_{m} down to the $0.006\,\mathrm{R}\ln 2$ for $x = 0.30$ which points to the itinerant nature of the weak ferromagnetism in the vicinity of

the critical concentration. Note that a magnetic entropy equal to zero is expected for an ideal itinerant electron ferromagnet[56]. Our results of the temperature dependence of the electrical resistivity provide evidence for a NFL behavior in the vicinity of x_{cr} most likely caused by the possible presence of the FM QCP. We have observed a drop of the n exponent in the temperature dependence of resistivity $\rho = \rho_0 + AT^n$ and an almost logarithmic dependence of the heat capacity $C(T)/T = c\ln(T_0/T)$ in a limited interval at lowest temperatures that would be in agreement with the theoretical predictions of Millis and Hertz[41,42]. Further evidence for the FM QCP is offered by the rapid increase of the effective mass of the quasiparticles near x_{cr}. The proposed scenario is also corroborated by scaling of the ordering temperature with the control parameter itself which obeys the formula $T_C \sim (x_{cr} - x)^{3/4}$ and provides estimation of the critical concentration $x_{cr} \approx 0.31$.

The FM transition of $UCo_{1-x}Ru_xGe$ compounds in the vicinity of x_{cr} is apparently of a second order type in contrast to the first order transition reported for 3-dimensional ferromagnets in the vicinity of a QCP[69]. Microscopic NQR studies of UCoGe suggest a first order transition to the FM state[70]. The second order transition in $UCo_{1-x}Ru_xGe$ compounds near x_{cr} can be conceived as a consequence of the substitution- induced disorder in the system which may blur the first order transition towards a continuous second order transition. In this context, we would like to mention the experimental and theoretical arguments regarding the observed anomalies related to the existence of a ferromagnetic QCP in $UCo_{1-x}Ru_xGe$ should be considered with a proper caution. Disorder caused by substitution can in some cases emulate NFL behavior[71,72] and may be one of the reasons of the lacking superconductivity in $UCo_{1-x}Ru_xGe$ in the proximity of the QCP. Thorough the investigation of single crystals of $UCo_{1-x}Ru_xGe$ compounds near x_{cr} at ambient and high pressures is highly desired in order to clarify the origin of the NFL state and the character of the ferromagnetic quantum phase transition in $UCo_{1-x}Ru_xGe$.

V. CONCLUSIONS

We have successfully prepared series of the polycrystalline samples of UCoGe doped with Ru in a wide range of concentration $UCo_{1-x}Ru_xGe$ ($0 \geq x \leq 0.9$). The Ru substitution leads to development of a FM dome between $x = 0 - 0.31$ with the maximum of $T_C = 8.6$ K and $M_S = 0.1\,\mu_B$ appearing at the $x \approx 0.1$. Further increase of the Ru content up to the critical concentration $x_{cr} \approx 0.31$ leads to the disappearance of the ferromagnetic state at a QCP. Using electronic structure calculations we were able to explain the evolution of ferromagnetism with x for $UCo_{1-x}Ru_xGe$ in terms of changes of the density of states at the Fermi level due to varying $5f$-ligand hybridization. The analysis of the critical exponents of the electrical resistivity and heat capacity at low temperatures revealed a non-Fermi liquid behavior for the samples in the vicinity of the QCP. The NFL state can be influenced by the substitution-induced disorder of the system because of the non-isoelectronic mixture of the $3d$ (Co) and $4d$ (Ru) bands. Further study of the region around the critical concentration including the measurements under the external pressure performed on high quality single crystals is highly desired for a better understanding the physics underlying the ferromagnetic quantum phase transition.

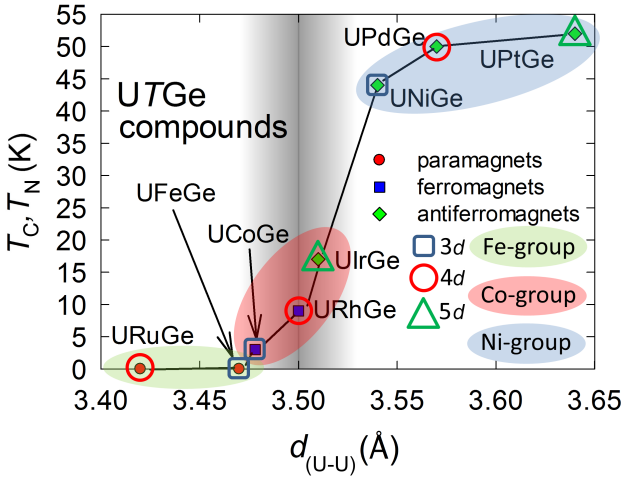

Figure 11. (Color online) - Illustrative plot showing the dependence of the ordering temperature of the UTGe compounds (T= transition metal) on the shortest distance between two nearest uranium atoms (d_{U-U}). Shaded region spreads around Hill limit (3.5 Å)[59] valid for uranium. Position of UFeGe is exceptional because UFeGe does not keep the TiNiSi-type structure[31].

ACKNOWLEDGMENTS

This work was supported by the Czech Science Foundation no. P204/12/P418 and the Charles University in Prague, project GA UK No.720214. Experiments performed in MLTL (see: http://mltl.eu/) were supported within the program of Czech Research Infrastructures (project LM2011025).

* michal.valiska@gmail.com

[1] S. S. Saxena, P. Agarwal, K. Ahilan, F. M. Grosche, R. K. W. Haselwimmer, M. J. Steiner, E. Pugh, I. R.

Walker, S. R. Julian, P. Monthoux, G. G. Lonzarich, A. Huxley, I. Sheikin, D. Braithwaite, and J. Flouquet, Nature **406**, 587 (2000).
[2] A. Huxley, I. Sheikin, E. Ressouche, N. Kernavanois, D. Braithwaite, R. Calemczuk, and J. Flouquet, Physical Review B **63**, 144519 (2001).
[3] D. Aoki, A. Huxley, E. Ressouche, D. Braithwaite, J. Flouquet, J.-P. Brison, E. Lhotel, and C. Paulsen, Nature **413**, 613 (2001).
[4] N. T. Huy, A. Gasparini, D. E. de Nijs, Y. Huang, J. C. P. Klaasse, T. Gortenmulder, A. de Visser, A. Hamann, T. Gorlach, and H. von Lohneysen, Physical Review Letters **99**, 067006 (2007).
[5] M. Uhlarz, C. Pfleiderer, and S. M. Hayden, Physical Review Letters **93**, 256404 (2004).
[6] D. E. de Nijs, N. T. Huy, and A. de Visser, Physical Review B **77**, 140506R (2008).
[7] C. Stock, D. A. Sokolov, P. Bourges, P. H. Tobash, K. Gofryk, F. Ronning, E. D. Bauer, K. C. Rule, and A. D. Huxley, Physical Review Letters **107**, 187202 (2011).
[8] T. Hattori, Y. Ihara, Y. Nakai, K. Ishida, Y. Tada, S. Fujimoto, N. Kawakami, E. Osaki, K. Deguchi, N. K. Sato, and I. Satoh, Physical Review Letters **108** (2012).
[9] D. v. d. Marel, H. J. A. Molegraaf, J. Zaanen, Z. Nussinov, F. Carbone, A. Damascelli, H. Eisaki, M. Greven, P. H. Kes, and M. Li, Nature **425**, 271 (2003).
[10] C. Pfleiderer, G. J. McMullan, S. R. Julian, and G. G. Lonzarich, Physical Review B **55**, 8330 (1997).
[11] A. Schroder, G. Aeppli, R. Coldea, M. Adams, O. Stockert, H. v. Lohneysen, E. Bucher, R. Ramazashvili, and P. Coleman, Nature **407**, 351 (2000).
[12] H. v. Lohneysen, T. Pietrus, G. Portisch, H. G. Schlager, A. Schroder, M. Sieck, and T. Trappmann, Physical Review Letters **72**, 3262 (1994).
[13] J. Custers, P. Gegenwart, H. Wilhelm, K. Neumaier, Y. Tokiwa, O. Trovarelli, C. Geibel, F. Steglich, C. Pepin, and P. Coleman, Nature **424**, 524 (2003).
[14] C. Pfleiderer and A. D. Huxley, Physical Review Letters **89**, 147005 (2002).
[15] D. Belitz, T. R. Kirkpatrick, and T. Vojta, Physical Review Letters **82**, 4707 (1999).
[16] V. P. Mineev, Comptes Rendus Physique **12**, 567 (2011).
[17] M. Janoschek, M. Garst, A. Bauer, P. Krautscheid, R. Georgii, P. Boni, and C. Pfleiderer, Physical Review B **87**, 134407 (2013).
[18] A. Menovsky, F. R. de Boer, P. H. Frings, and J. J. M. Franse, in *High Field Magnetism*, edited by M. Date (Elsevier, Amsterdam, 1983) pp. 189–191.
[19] M. Sutherland, R. P. Smith, N. Marcano, Y. Zou, S. E. Rowley, F. M. Grosche, N. Kimura, S. M. Hayden, S. Takashima, M. Nohara, and H. Takagi, Physical Review B **85**, 035118 (2012).
[20] D. Aoki and J. Flouquet, Journal of the Physical Society of Japan **81**, 011003 (2012).
[21] A. Gasparini, Y. K. Huang, N. T. Huy, J. C. P. Klaasse, T. Naka, E. Slooten, and A. de Visser, Journal of Low Temperature Physics **161**, 134 (2010).
[22] D. Aoki, T. D. Matsuda, V. Taufour, E. Hassinger, G. Knebel, and J. Flouquet, Journal of the Physical Society of Japan **78**, 113709 (2009).
[23] J. Pospisil, J. P. Vejpravova, M. Divis, and V. Sechovsky, Journal of Applied Physics **105**, 07E114 (2009).
[24] R. Troc and V. H. Tran, Journal of Magnetism and Magnetic Materials **73**, 389 (1988).
[25] N. T. Huy and A. de Visser, Solid State Communications **149**, 703 (2009).
[26] N. T. Huy, A. Gasparini, J. C. P. Klaasse, A. de Visser, S. Sakarya, and N. H. van Dijk, Physical Review B **75**, 212405 (2007).
[27] J. Pospisil, K. Prokes, M. Reehuis, M. Tovar, J. Poltierova Vejpravova, J. Prokleska, and V. Sechovsky, Journal of the Physical Society of Japan **80**, 084709 (2011).
[28] H. Rietveld, Journal of Applied Crystallography **2**, 65 (1969).
[29] J. Rodriguez-Carvajal, Physica B: Condensed Matter **192**, 55 (1993).
[30] T. Roisnel and J. Rodriguez-Carvajal (Trans Tech Publications).
[31] F. Canepa, P. Manfrinetti, M. Pani, and A. Palenzona, Journal of Alloys and Compounds **234**, 225 (1996).
[32] J. P. Perdew and Y. Wang, Physical Review B **45**, 13244 (1992).
[33] J. P. Perdew, K. Burke, and M. Ernzerhof, Physical Review Letters **77**, 3865 (1996).
[34] K. Schwarz, P. Blaha, and G. K. H. Madsen, Computer Physics Communications **147**, 71 (2002).
[35] L. Vegard, Zeitschrift fur Physik A Hadrons and Nuclei **5**, 17 (1921).
[36] B. Cordero, V. Gomez, A. E. Platero-Prats, M. Reves, J. Echeverria, E. Cremades, F. Barragan, and S. Alvarez, Dalton Transactions **0**, 2832 (2008).
[37] A. Arrott, Physical Review **108**, 1394 (1957).
[38] M. Valiska, J. Pospisil, A. Stunault, Y. Takeda, B. Gillon, Y. Haga, K. Prokes, M. M. Abd-Elmeguid, G. Nenert, T. Okane, H. Yamagami, L. Chapon, A. Gukasov, A. Cousson, E. Yamamoto, and V. Sechovsky, (2015), arXiv:1504.05645.
[39] K. Huang, J. J. Hamlin, R. E. Baumbach, M. Janoschek, N. Kanchanavatee, D. A. Zocco, F. Ronning, and M. B. Maple, Physical Review B **87**, 054513 (2013).
[40] J. Prokleska, J. Pospisil, J. Vejpravova Poltierova, V. Sechovsky, and J. Sebek, Journal of Physics: Conference Series **200**, 012161 (2010).
[41] A. J. Millis, Physical Review B **48**, 7183 (1993).
[42] J. A. Hertz, Physical Review B **14**, 1165 (1976).
[43] G. R. Stewart, Reviews of Modern Physics **73**, 797 (2001).
[44] A. Gasparini, Y. K. Huang, J. Hartbaum, H. von Lohneysen, and A. de Visser, Physical Review B **82**, 052502 (2010).
[45] M. Divis, Physica B-Condensed Matter **403**, 2505 (2008).
[46] M. B. S. Neto, A. H. C. Neto, J. S. Kim, and G. R. Stewart, Journal of Physics: Condensed Matter **25**, 025601 (2013).
[47] C. D. Batista, J. Bonca, and J. E. Gubernatis, Physical Review Letters **88**, 187203 (2002).
[48] C. D. Batista, J. Bonca, and J. E. Gubernatis, Physical Review B **68**, 214430 (2003).
[49] T. Gasche, M. S. S. Brooks, and B. Johansson, Journal of Physics: Condensed Matter **7**, 9499 (1995).
[50] D. M. Newns and N. Read, Advances in Physics **36**, 799 (1987).
[51] T. Moriya, (Springer Berlin Heidelberg, 2012).
[52] J. L. Smith and E. A. Kmetko, Journal of the Less Common Metals **90**, 83 (1983).
[53] B. R. Cooper, Q. G. Sheng, S. P. Lim, C. Sanchez-Castro, N. Kioussis, and J. M. Wills, Journal of Magnetism and Magnetic Materials **108**, 10 (1992).
[54] M. S. S. Brooks and P. J. Kelly, Physical Review Letters **51**, 1708 (1983).

[55] G. H. Lander, M. S. S. Brooks, and B. Johansson, Physical Review B **43**, 13672 (1991).
[56] V. Sechovsky and L. Havela, in *Handbook of Magnetic Materials*, Vol. Volume 11, edited by K. H. J. Buschow (Elsevier, 1998) pp. 1–289.
[57] C. Sanchez-Castro, B. R. Cooper, and K. S. Bedell, Physical Review B **51**, 12506 (1995).
[58] M. Taupin, J.-P. Brison, D. Aoki, J.-P. Sanchez, F. Wilhelm, and A. Rogalev, ArXiv e-prints (2015).
[59] H. H. Hill, pp. 1 – 19.
[60] M. Wulff, G. H. Lander, B. Lebech, and A. Delapalme, Physical Review B **39**, 4719 (1989).
[61] R. Troc, V. H. Tran, F. G. Vagizov, and H. Drulis, Journal of Alloys and Compounds **200**, 37 (1993).
[62] P. A. Veenhuizen, F. R. de Boer, A. A. Menovsky, V. Sechovsky, and L. Havela, Journal de Physique **49**, 485 (1988).
[63] O. Eriksson, B. Johansson, and M. S. S. Brooks, Journal of Physics: Condensed Matter **1**, 4005 (1989).
[64] M. Shimizu, J. Phys. France **43**, 155 (1982).
[65] N. V. Mushnikov, T. Goto, K. Kamishima, H. Yamada, A. V. Andreev, Y. Shiokawa, A. Iwao, and V. Sechovsky, Physical Review B **59**, 6877 (1999).
[66] A. V. Andreev, L. Havela, V. Sechovsky, M. I. Bartashevich, J. Sebek, R. V. Dremov, and I. K. Kozlovskaya, Philosophical Magazine B-Physics of Condensed Matter Statistical Mechanics Electronic Optical and Magnetic Properties **75**, 827 (1997).
[67] V. Sechovsky, L. Havela, F. R. de Boer, P. A. Veenhuizen, K. Sugiyama, T. Kuroda, E. Sugiura, M. Ono, M. Date, and A. Yamagishi, Physica B: Condensed Matter **177**, 164 (1992).
[68] N. V. Mushnikov, T. Goto, A. V. Andreev, V. Sechovsky, and H. Yamada, Physical Review B **66**, 064433 (2002).
[69] D. Belitz and T. R. Kirkpatrick, (2012), arXiv:1204.0873.
[70] T. Hattori, K. Ishida, Y. Nakai, T. Ohta, K. Deguchi, N. K. Sato, and I. Satoh, Physica C: Superconductivity **470**, S561 (2010).
[71] E. Miranda, V. Dobrosavljevic, and G. Kotliar, Physical Review Letters **78**, 290 (1997).
[72] A. Rosch, Physical Review Letters **82**, 4280 (1999).